

**Investigations of turbulence in a liquid helium II counterflow jet**

Paul E. Dimotakis and Glenn A. Laguna\*

*California Institute of Technology, Pasadena, California 91125*

(Received 8 July 1976; revised manuscript received 24 January 1977)

Using the phase information in a high-frequency second-sound beam, it was possible to investigate the temperature and velocity in a counterflow jet a few diameters downstream of the jet exit. At the heat fluxes investigated, the jet was characterized by turbulent velocity fluctuations. No temperature difference could be measured between the jet and the surrounding fluid, within the experimental accuracy ( $\sim 10^{-5}$  K). Velocity-sensitive phase measurements suggest that the normal-fluid jet entrains the surrounding superfluid to minimize any relative velocity and mutual friction between the two fluids. To our knowledge these observations constitute the first direct measurements of liquid-helium fluid velocities, as they enter the equations of motion.

I. INTRODUCTION

Recent experimental investigations<sup>1-3</sup> of the counterflow jet,<sup>4</sup> in liquid helium II, raise several questions about the mutual friction<sup>5</sup> between the two fluids. The results of these investigations seem to suggest that, in the jet, either the mutual friction is not operative, or that the relative velocity between the fluids is zero (or subcritical). The former case would lend support to the notion that the mutual-friction mechanism requires the presence of walls, while the second case would require that the normal fluid entrain the superfluid. Matters are further complicated as a result of ion-transport experiments<sup>6</sup> which indicate that vortex lines, which are considered necessary for mutual friction<sup>7</sup> are actually present in the counterflow jet.

To investigate these questions, and jet flow in liquid helium II in general, we took advantage of the dependence of the velocity of second sound on the mass-flux velocity

$$\vec{v} = (\rho_n \vec{v}_n + \rho_s \vec{v}_s) / \rho, \tag{1}$$

the relative velocity between the normal fluid and superfluid

$$\vec{w} = \vec{v}_n - \vec{v}_s, \tag{2}$$

and temperature. In particular, to first order in  $\vec{v}$  and  $\vec{w}$ , Khalatnikov<sup>8</sup> predicted that

$$u_{II}^{(0)}(p, T) = v_k + f(p, T)w_k, \tag{3}$$

where  $v_k$  and  $w_k$  are the components of the mass-flux velocity and relative velocity, along the second-sound wave vector, and  $u_{II}^{(0)}(p, T)$  is the second-sound velocity in the fluid at rest,

$$u_{II}^{(0)}(p, T) = (\rho_s s^2 T / c\rho_n)^{1/2}. \tag{4}$$

The dimensionless coefficient  $f(p, T)$  is given by<sup>8</sup>

$$f(p, T) = 2 \frac{\rho_s}{\rho} - \frac{s}{c\rho_n} \left( \frac{\partial \rho_n}{\partial T} \right)_p \tag{5}$$

and plotted in Fig. 1, along the saturated vapor-pressure curve. These predictions have been verified experimentally by Johnson and Hildebrand<sup>9</sup> in pure counterflow ( $v=0$ ), in the temperature range 1.30–1.95 K.

The principle of the measurement technique can be described as follows. Assume a plane running wave beam within a plane parallel emitter detector pair spaced by a distance  $D$ . The phase of the wave at the detector is given by the line integral of the second sound wave vector, i.e.,

$$\phi = \int_0^D \vec{k} \cdot d\vec{x},$$

where the magnitude of  $\vec{k}$  is given by

$$k = |\vec{k}| = \omega / u_{II},$$

and  $\omega$  is the angular frequency of the wave. If we

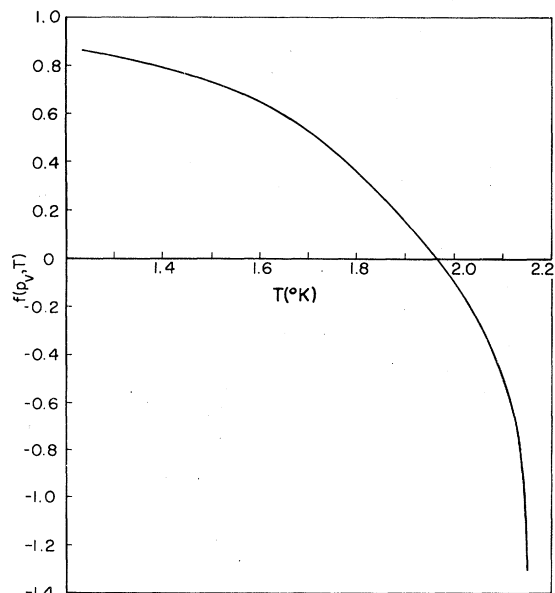


FIG. 1.  $f(p, T)$  along vapor-pressure curve.

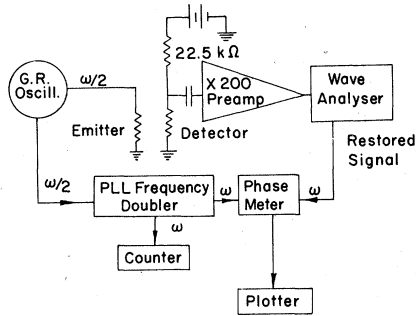


FIG. 2. Signal-processing electronics block diagram (G. R., General Radio; PLL, phase locked loop).

assume that the fluid is quiescent, except for a bounded perturbed region of extent  $L$  along the wave vector, we have

$$\phi = \phi_0 + \Delta\phi, \quad (6)$$

where

$$\phi_0 = \omega D / u_{II}^{(0)}(p, T) \quad (6a)$$

and, to first order in the perturbations,

$$\Delta\phi = \frac{-\omega L}{[u_{II}^{(0)}(p, T)]^2} \left( \bar{v}_k + f(p, T) \bar{w}_k + \frac{\partial u_{II}^{(0)}}{\partial T} \delta \bar{T} \right). \quad (6b)$$

The quantities  $\bar{v}_k$ ,  $\bar{w}_k$ , and  $\delta \bar{T}$  are the averages of the corresponding local values in the perturbed region, along the path of the second-sound beam.

The different parts of the phase shift can be measured by introducing and removing the disturbance sequentially and measuring the resulting phase difference. This technique was used to investigate several aspects of the counterflow jet which will be discussed below.

## II. EXPERIMENTAL TECHNIQUE AND INSTRUMENTATION

In practice, the emitter dimensions, as scaled by the second-sound wavelength, must be large enough to generate a collimated plane-wave diffraction-limited beam. The sensing part of the beam, however, as defined by the emitter-detector combination, must be small enough to meet the desired spatial-resolution requirements. The frequency must be chosen to be sufficiently high for the second-sound volume attenuation in an emitter-detector round trip to be large enough to eliminate standing wave, Fabry-Perot type resonances.<sup>2,3,10</sup> This ensures a pure running-wave second-sound beam from the emitter to the detector. Yet the frequency must not be so high as to allow the volume attenuation to reduce the temperature amplitude of the wave at the detector to below desired detectable levels. These consider-

ations dictate second-sound frequencies of several hundred kilohertz. The selected emitter detector spacing was 5 cm. The sensing beam cross section, as defined by the detector sensing element, was square, 1 mm on the side. The techniques of generation and detection of second sound with these specifications have been documented elsewhere.<sup>2,3,10,11</sup>

The second-sound emitter was driven by a General Radio model 1310-B oscillator, at half the second-sound frequency, which also provided an input to a phase-locked loop frequency doubler. The detector signal was amplified by a matched 50- $\Omega$  impedance 46-dB preamplifier with a noise figure of 0.6 nV/(Hz)<sup>1/2</sup>. The preamplifier output was processed by a Hewlett-Packard model 3590 wave analyzer operated in the automatic-frequency-control mode with a 3.1-kHz bandwidth. Finally, the phase was measured on a Wavetek model 740 phase meter by comparing the restored signal output from the wave analyzer to the square-wave reference signal provided by the phase-locked frequency doubler. A block diagram of the second-sound generation and signal-processing scheme appears in Fig. 2. A sensitivity of 0.6 V/K of the detector, the preamp noise figure and the wave analyzer bandwidth combined to yield an equivalent noise temperature at the detector of the order of  $6 \times 10^{-8}$  K. The frequency doubled square wave and the detected second-sound signal output from the wave analyzer are shown in Fig. 3. The high signal-to-noise ratio of the detected second sound is quite evident. The second-sound frequency is 500 kHz.

## III. TEMPERATURE-SENSITIVE PHASE MEASUREMENTS

The dependence of the detected phase on the mean temperature difference  $\delta \bar{T}$  of the perturbed

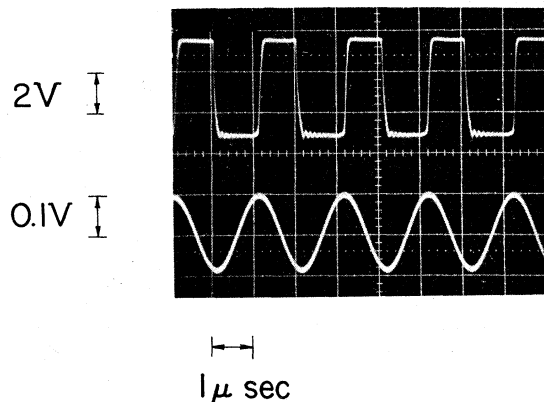


FIG. 3. Frequency doubled reference (square wave) and detected second-sound signal at 500 kHz.

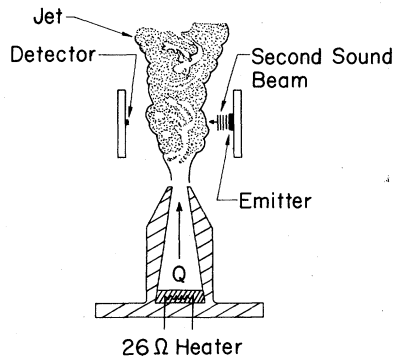


FIG. 4. Second-sound beam and jet geometry for temperature measurement.

region with respect to the quiescent region [Eq. 6(b)] renders this technique a very accurate way of measuring the temperature of the jet from a distance, without the undesirable disturbances of a material probe. In addition, if the phase measurements are to be used to extract information about the flow velocities, the contribution due to temperature differences must either be known, or the measurements must be performed within a temperature interval where  $\partial u_{II}^{(0)}/\partial T$  is acceptably small.

The geometrical arrangement for this measurement is depicted in Fig. 4. The interior of the counterflow jet was axisymmetric with an  $8^\circ$  contraction half-angle and a diameter at the exit of  $d=0.64$  cm. A  $26\text{-}\Omega$  Evanohm wire heater potted in Wood's metal to assure a uniform heat flux drove the counterflow. The ratio of the area at the heater to that at the exit was approximately 10.5. The second-sound beam crossed the jet at right angles to its axis ( $\bar{v}_k = \bar{w}_k = 0$ ) approximately 3.2 cm downstream of the exit corresponding to an  $x/d \approx 5$ . The different parts of the phase, i.e.,  $\phi_0$  as given by Eq. (6a) and  $\Delta\phi$  as given by Eq. (6b), could be measured separately by turning the jet on and off. The temperature of the bath was regulated quite simply but very effectively by controlling the vapor pressure with a condom pressure regulator.<sup>1,2,12</sup> To maintain a constant load on the regulator, a dummy matched heater in the bath was switched off as the counterflow heater was switched on and vice versa. An example of the resulting phase measurement is shown in Fig. 5, plotted versus time to facilitate the removal of the effect of small temperature drifts in the system. The bath temperature for this measurement was 2.072 K and the jet heat flux was  $1.05\text{ W/cm}^2$ . The second-sound frequency was 500 kHz. Careful scrutiny of Fig. 5 discloses a barely discernible mean phase decrease during the time the jet is on. This is probably attributable to a slight deviation of the

free jet axis from the perpendicular (to the second-sound beam wave vector). Using Eq. (6b), with  $\bar{v}_k = \bar{w}_k = 0$ , and even assuming that at  $x/d \approx 5$  the jet has not spread appreciably, we compute that a  $\delta T \sim 10^{-5}$  K in the jet would have resulted in a  $\Delta\phi \sim 3^\circ$  at  $T=2.072$  K, where  $\partial u_{II}^{(0)}/\partial T$  is negative. Consequently, if there exists a temperature difference between the jet column and the surrounding fluid it is less than or, at most, of the order of  $10^{-5}$  K at these conditions. This conclusion is in agreement with previous measurements<sup>1,3</sup> in the jet and places a considerably lower upper bound on any possible temperature difference than had been established before.

While for this beam orientation the mean values of  $v_k$  and  $w_k$  are zero by symmetry, fluctuations in these quantities can give instantaneous contributions to the phase shift introduced by the jet. The substantial phase fluctuations, that are evident in Fig. 4 when the jet is on, indicate that the flow is turbulent.

#### IV. VELOCITY-SENSITIVE PHASE MEASUREMENTS

Having established that, within experimental error, the jet column possesses the same temperature as the surrounding fluid, the second-sound beam was tilted to render the phase measurements sensitive to velocities in the jet. For the remainder of the data presented here, the beam formed a  $60^\circ$  angle with respect to the jet axis crossing it at an  $x/d \approx 5$ , as before. See Fig. 6. Sample phase measurements are plotted in Fig. 7 for a relatively high heat flux of  $1.05\text{ W/cm}^2$ . The effect of the jet on the phase is quite well defined. The bath temperature for this run was 1.706 K and the second-sound frequency was 250 kHz. The phase fluctuations associated with the jet are quite large indicating, as before, that the flow is turbulent. It should be noted that this observation

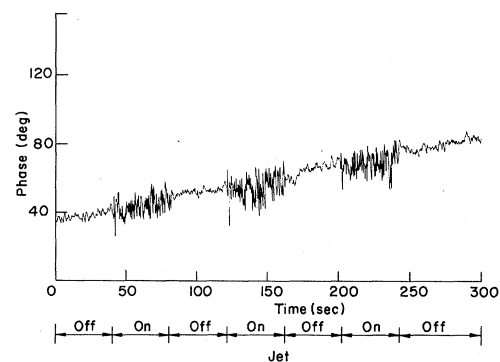


FIG. 5. Temperature measurement in the counterflow jet using high-frequency second sound.  $T=2.072$  K,  $\bar{q}=1.05\text{ W/cm}^2$ ,  $x/d \approx 5$ ,  $\nu=500$  kHz.

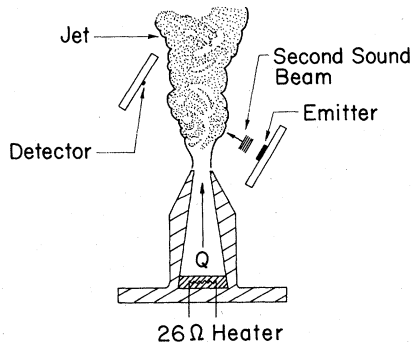


FIG. 6. Velocity-sensitive phase-measurement geometry.

is in agreement with Kapitza's experiments in the counterflow jet.<sup>4</sup> He found what could be identifiable as a laminar-turbulent transition on the jet, at an  $x/d$  which was a function of the heat flux (Reynolds number). This behavior is consistent with classical jet behavior,<sup>13</sup> which would also indicate that our much higher Reynolds-number jet is essentially turbulent from the outset.

From data such as in Fig. 7, the mean phase shift due to the jet can be measured as a function of the heat flux. Examples of such data are plotted in Figs. 8, 9, and 10, for bath temperatures of 1.594, 1.929, and 2.077 K, respectively. The vertical bars of the plotted points represent an estimate of the peak fluctuation level of the measured phase shift due to the jet.

To provide a basis for comparison, the expected phase shift is also indicated (dashed lines) computed on the basis of Eq. (6b), corresponding to the following assumptions: (i) the net mass flux velocity component along the second-sound beam is zero ( $\bar{v}_k = 0$ ); (ii) the mean relative velocity component, along the second-sound beam ( $\bar{w}_k$ ), is

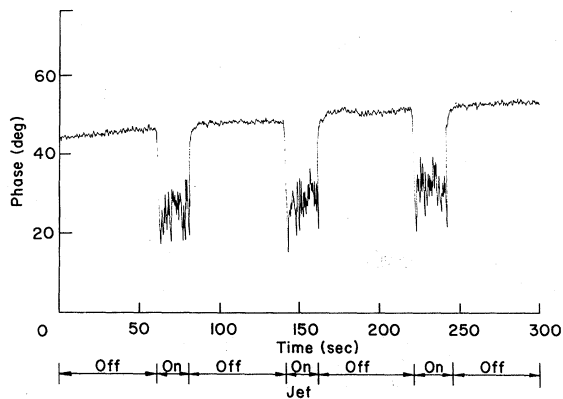


FIG. 7. Velocity-sensitive phase measurements. Bath temperature is 1.706 K. Heat flux is 1.05 W/cm<sup>2</sup>. Second-sound frequency is 250 kHz. Beam angle with respect to jet axis is 60°.

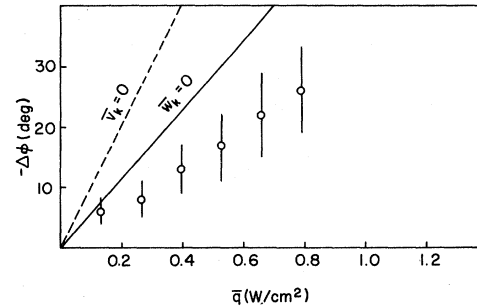


FIG. 8. Phase shift vs heat flux.  $T=1.594$  K,  $\nu=250$  kHz, beam angle is 60°.

equal to its value at the jet exit, or

$$\bar{w} = \bar{q} / \rho_s s T,$$

where  $\bar{q}$  is the mean heat flux through the jet exit; and (iii) the jet has not spread appreciably by  $x/d \sim 5$ . As can be seen, the phase shifts computed from this model are in disagreement with even the qualitative behavior of the measurements, as a function of temperature.

The expected phase shift was also computed (solid lines) on the basis of the following assumptions: (a) the mean relative velocity component along the second-sound beam is zero ( $\bar{w}_k = 0$ ); (b) the mean mass flux velocity component along the second-sound beam ( $\bar{v}_k$ ) is such as to conserve the momentum flux of the jet, i.e.,

$$J = (\rho \bar{v}^2)_{x/d \sim 5} = \left( \frac{\rho_n \bar{D}_s}{\rho} \bar{w}^2 \right)_{\text{exit}},$$

and therefore,

$$\bar{v} = \left( \frac{\rho_n}{\rho} \right)^{1/2} \left( \frac{\rho_s}{\rho} \right)^{1/2} \frac{\bar{q}}{\rho_s s T};$$

(c) the jet does not spread; and (d) the velocity is constant within the jet column (and zero outside). From the improved qualitative agreement, it would appear that this model is a closer representation of the actual flow field. Unfortunately, a more

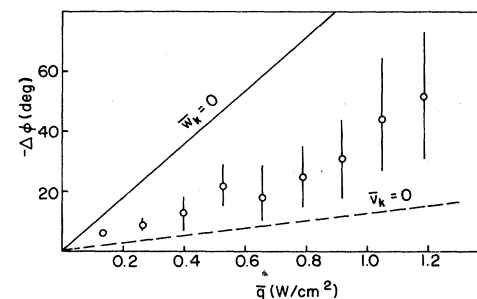


FIG. 9. Phase shift vs heat flux.  $T=1.929$  K,  $\nu=500$  kHz, beam angle is 60°.

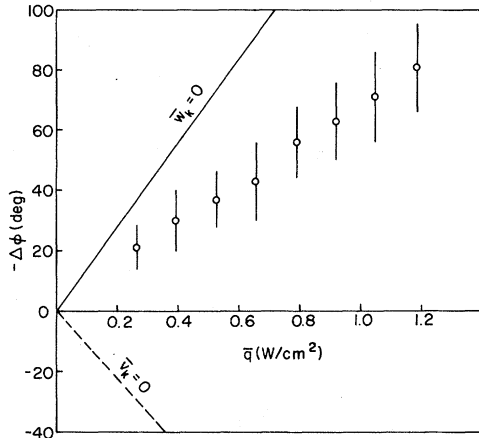


FIG. 10. Phase shift vs heat flux.  $T=2.077$  K,  $\nu=500$  kHz, beam angle is  $60^\circ$ .

realistic calculation requires detailed knowledge of the velocity profiles for the two fluids. The obvious complexity, however, of the flow pattern, suggested by the present measurements, discourages us from attempting precise calculations, at the present, based on *ad hoc* assumptions.

## V. CONCLUSION

High-frequency second-sound phase measurements across a counterflow jet have shown the flow to be turbulent at high-heat fluxes. Temperature-sensitive phase measurements could not establish any temperature difference between the jet and the surrounding fluid, within the experimental resolution ( $<10^{-5}$  K). Velocity sensitive phase measurements, even though not quite definitive, are consistent with the notion that the normal fluid jet entrains the surrounding superfluid to minimize the relative velocity between the two fluids. This, in turn, suggests that the mutual friction is operative in the jet and provides the force that drags the superfluid along. The relative velocity required to sustain this flow pattern is probably too small to result in any measurable frictional effects (temperature gradients, additional second-sound attenuation, etc.).

## ACKNOWLEDGMENT

The authors would like to thank the Air Force Office of Scientific Research for supporting this work through contract No. F44620-75-C-0038.

\*Presently at: Yale University, New Haven, Conn. 06520.

<sup>1</sup>P. E. Dimotakis and J. E. Broadwell, *Phys. Fluids* **16**, 1787 (1973).

<sup>2</sup>G. A. Laguna, Ph.D. thesis (California Institute of Technology, 1975) (unpublished).

<sup>3</sup>G. A. Laguna, *Phys. Rev. B* **12**, 4874 (1975).

<sup>4</sup>P. L. Kapitza, *J. Phys. USSR* **4**, 181 (1941).

<sup>5</sup>C. J. Gorter and J. H. Mellink, *Physica (Hague)* **15**, 285 (1949).

<sup>6</sup>G. Careri, M. Cerdonio, and F. Dupr e, *Phys. Rev.*

*167*, 233 (1968).

<sup>7</sup>W. F. Vinen, *Proc. R. Soc. Lond. A* **242**, 493 (1957).

<sup>8</sup>I. M. Khalatnikov, *Sov. Phys.-JETP* **3**, 649 (1956).

<sup>9</sup>E. M. Johnson and A. F. Hildebrandt, *Phys. Rev.* **178**, 292 (1969).

<sup>10</sup>H. A. Notarys, Ph.D. thesis (California Institute of Technology, 1964) (unpublished).

<sup>11</sup>G. A. Laguna, *Cryogenics* **16**, 241 (1976).

<sup>12</sup>H. A. Notarys (private communication).

<sup>13</sup>K. J. McNaughton and C. G. Sinclair, *J. Fluid Mech.* **25**, 367 (1966).

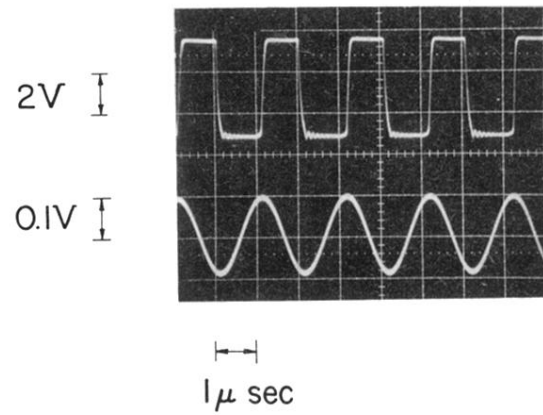


FIG. 3. Frequency doubled reference (square wave) and detected second-sound signal at 500 kHz.